

We are IntechOpen, the world's leading publisher of Open Access books Built by scientists, for scientists

4,800

Open access books available

122,000

International authors and editors

135M

Downloads

Our authors are among the

154

Countries delivered to

TOP 1%

most cited scientists

12.2%

Contributors from top 500 universities



WEB OF SCIENCE™

Selection of our books indexed in the Book Citation Index
in Web of Science™ Core Collection (BKCI)

Interested in publishing with us?
Contact book.department@intechopen.com

Numbers displayed above are based on latest data collected.
For more information visit www.intechopen.com



Antennas and Front-End in GNSS

Korkut Yegin

Additional information is available at the end of the chapter

<http://dx.doi.org/10.5772/intechopen.74971>

Abstract

Antenna and front-end play a key role in global navigation satellite system (GNSS) receivers where multi-frequency and multi-constellation services are used simultaneously to produce high-precision position, navigation, and timing information. Being the first element on the receiver system, specifications on the antenna for multi-constellation GNSS applications can be challenging. Especially, integration of the antenna into the target platform, either mobile or stationary, may severely affect antenna performance. This is usually an issue for small-size antennas where measured stand-alone antenna performance in ideal conditions is usually not descriptive of actual performance on the platform. Furthermore, carrier phase tracking has become popular among algorithm developers to obtain high accuracy and anti-spoofing at the same time which demand minimal phase centre variation of the antenna within the intended GNSS band. Spoofing and jamming of GNSS receivers is a growing concern especially for aerial vehicles with ever-increasing applications of drones. These requirements demand different characteristics on the antenna and front-end than traditional applications. One of the most utilized forms of GNSS antenna is ceramic patch, due to its low height, low cost, and relatively good narrow band performance. Simulations of this particular antenna in terms of axial ratio and impedance bandwidths, axial ratio variation over elevation, and half-power beam width are carried out and discussed with comparison to its counterparts. Another critical part of the receiver is its front-end where huge amount of signal amplification with minimal distortion takes place. Long integration times (>1 ms) in GNSS signal processing also puts severe requirements on the software and temperature-compensated crystal oscillator. For mass production, the front-end should be implemented in the form of an integrated circuit. Front-end architectures from traditional superheterodyne to zero/low-intermediate frequency configurations are presented. Advantages and disadvantages of each configuration are outlined in view of multi-band and multi-standard GNSS receivers.

Keywords: GNSS antenna, carrier phase tracking, GNSS low-noise amplifier, GNSS front-end, low-IF receiver

1. Introduction

Global navigation satellite systems (GNSSs) are indispensable in positioning, navigation, and timing (PNT) and have become an integral part of many outdoor positioning applications such as surveying, vehicle localization, parcel and container tracking, precision timing, synchronization of communication networks and radars, atmospheric observation, and meteorology. Although GNSS has started with US Global Satellite System (GPS) only, with the addition of new GNSS services introduced by Russia, China, and European Union, GNSS has evolved to multi-constellation and multi-band system. Regional satellite navigation system by India and GNSS assistance services such as QRZZ also complement global satellite navigation system. All global service providers of GNSS offer worldwide positioning for mobile and stationary platforms and assets.

While multiple GNSS services at different frequency bands offer tremendous advantages for the user which were not possible with single service provider, multi-band and multi-constellation receivers and antennas possess new challenges in the system design. For precise positioning, multiple satellites, at least four for each service provider, must be tracked simultaneously. One of the key components of the system is the GNSS passive antenna, which is vital to establish a good carrier-to-noise ratio for seamless positioning with minimum acquisition time. The antenna beam width must be broad to cover as much as possible the sky view while its axial ratio must be low throughout its coverage. The antenna must maintain these features throughout the target frequency bands. The receiver, on the other hand, must be able to handle multi-constellation GNSS signals. Instead of classical receiver architectures, software-defined, user-configurable GNSS architectures are much more in demand due to the flexibility in software they offer.

One of the key challenges in any GNSS is the susceptance of receiver to interference. The signals transmitted through satellites are at low power such that the received signals are very weak on earth and usually under the thermal noise floor of the receiver. Intentional and unintentional jamming of GNSS signals is common and still presents the biggest problem in GNSS applications. Especially, in urban environment where tall buildings block clear view of the antenna and multipath propagation is dominant, the receiver performance deteriorates significantly. Unintentional blockage of GNSS due to other communication systems is also common. Strong out-of-band signals or signal bleeding from nearby frequency bands can cause interruptions of GNSS service. Due to very weak signal levels on earth, intentional jamming with inexpensive hardware has also proven to be harmful for GNSS service. Jamming mitigation at the hardware and software are essential components of the mission-critical GNSS receivers.

2. GNSS passive antenna

Since the inception of GPS, satellite navigation antenna, maybe, is one of the most studied antenna structures in the literature. It is difficult to give a comprehensive list, but microstrip

patch antennas and antenna performance on the platform [1–7], wideband antennas [8, 9], wide beam width antenna [10], miniature and multi-functional antennas [11–18], dual/triple GNSS band antennas [19–25], conformal and missile application antennas [26–29], array antennas for anti-jam and anti-spoofing applications [30–35], cellular phone isolation [36, 37], metamaterial and plasma-supported antennas [38–41] are reported in the literature.

Depending on the antenna location inside the platform and available antenna space, antenna designers routinely face challenges to meet acceptable performance. Most utilized forms of GNSS antennas are microstrip antennas, helical antennas, slot-based antennas and miniature (chip-scale) antennas. GNSS antenna arrays are often essential for critical applications where precise positioning is required along with counter measures for jamming and spoofing.

2.1. GNSS passive antenna requirements

GNSS passive antenna performance is usually quantified in terms of operational frequency band, gain pattern, half-power beam width (HPBW), polarization, axial ratio, cross-polarization discrimination or multipath discrimination, and phase centre stability.

2.1.1. Operational frequency band

The passive antenna must be functional within the desired GNSS service band. The operation frequencies of current GNSS services are tabulated in **Table 1**. A passive antenna that is capable of receiving entire GNSS services must be operational from 1164 to 1610 MHz (32.1% fractional bandwidth), covering either entire band or multi-band within lower L-band (1164–1300 MHz) and upper L-band (1559–1610 MHz).

2.1.2. Polarization

L-band satellite navigation systems utilize right-hand circular polarization (RHCP) signals. Two orthogonal components of circular polarization signal at high elevations undergo same level of Faraday rotation when passing through ionosphere which does not degrade the

Service	Lower L-band	Upper L-band
GPS	L5: 1164–1189 MHz L2: 1215–1239.6 MHz	L1: 1567–1587 MHz
Galileo	E5: 1164–1215 E6: 1260–1300 MHz	E1: 1559–1591
GLONASS	G3: 1189–1214 MHz G2: 1237–1254 MHz	G1: 1593–1610 MHz
BeiDou/compass	B2I: 1179–1203 MHz B3: 1256–1280	B1I: 1553–1569 MHz

Table 1. GNSS frequency bands.

polarization purity of the signal. For linearly polarized signals, Faraday rotation causes the signal to a different tilt angle than the original which should be compensated at the receiving antenna on earth either by rotating the antenna to correct polarization or utilizing both orthogonal components of the received signal for polarization compensation.

2.1.3. Axial ratio and multipath rejection

The purity of a circular polarization is stated in terms of axial ratio (AR), which is defined as the ratio of two orthogonal components of electric field on polarization ellipse traced by the electric field vector in time domain. Axial ratio changes with elevation and azimuth, but it is usually stated at zenith as a single value. Good GNSS antennas usually have less than 1 dB axial ratio at zenith, and moderate ones have less than 3 dB. Although it is possible to obtain low axial ratios at zenith, it is relatively difficult to achieve the same performance at low elevation angles. Most circularly polarized antenna structures are linearly polarized at low elevation angles, which make reception somewhat difficult but jamming and spoofing easy. Furthermore, it is also difficult to maintain the same axial ratio over a large bandwidth. Thus, axial ratio bandwidth is often the limiting factor than the impedance bandwidth for circularly polarized antennas.

Cross-polarization (X_{pol}) of the antenna is related to the axial ratio through the following equation:

$$X_{pol} = (AR - 1)^2 / (AR + 1)^2 \quad (1)$$

Thus, specification of axial ratio is sufficient to estimated cross-polarization level of the directly received signal. Upon reflection from a surface, the sense of polarization changes from right hand to left hand, thus good cross-polarization at the antenna leads to better rejection of multi-path signals. Multi-path rejection ratio (MPRR) of the antenna for ground reflection can be formulated as

$$MPRR_{dB} = 20 \log \left(\frac{E_{RHCP}(\theta)}{E_{RHCP}(180 - \theta) + E_{LHCP}(180 - \theta)} \right) \quad (2)$$

where $180 - \theta$ corresponds to the angle for the ground reflected signal.

2.1.4. Beam width and gain

HPBW is a good measure of antenna gain roll-off and sky coverage. It is usually desired to be in excess of 85° . For wider beam width ($>120^\circ$), the antenna gain must be compromised to lower values. This trade-off, sometimes, pays off depending on the platform where the antenna is mounted. However, larger beam width may be a disadvantage for spoofing countermeasures and antenna noise. Desired gain roll-off depends on the particular application and the platform where the antenna is situated.

Passive antenna gain is largely dependent on the choice of antenna structure which is usually dictated by the available space for the antenna. In space-constrained applications, the form factor antenna is so small that the expected gain can be as low as -5 dBic. Most fade margin

calculations assume 0 dBic antenna gain, but this can be difficult to achieve for a printed circuit board (PCB) or chip antenna. Moreover, these small, integrated antennas suffer non-uniform reception in the azimuth, making antenna reception dependent on the platform or user orientation.

2.1.5. Phase-centre stability

Electrical phase centre of the antenna is described as the geometrical point where all rays converge or emanate from it, i.e. incident rays add up in phase. Measured signals are all relative to this position, thus antenna phase centre plays a key role in achieving millimetre resolution in positioning. Although it is described as a single point in space, the phase centre changes with frequency. Within the respective GNSS band, a phase centre variation adds up to inaccuracies in pseudo-range calculation. Especially in an array configuration where the main lobe of the array is tilted to desired angle, phase centre may change depending on the tilt angle. Phase centre offset must be specified for every direction and frequency for accurate PNT estimation. In recent years, spoofing or interference detection based on received signal phase variation relies on phase-centre variation of the passive antenna. Less than 1 cm phase centre variation in transverse plane is usually acceptable, though smaller is better.

General technical specifications for a GNSS passive antenna are summarized in **Table 2**. It should be noted that these specification are by no means strict and can vary largely depending on the antenna platform and the specific application. For instance, mobile phone GNSS antenna specifications largely vary from that of a revolving missile guidance antenna or from a land-surveying antenna.

2.2. Microstrip antennas

Microstrip patch antennas are low-profile, easy to integrate, and relatively low cost. In most applications, the height of the antenna becomes the limiting factor in platform design. Although helical antennas, for instance, perform better than microstrip counterparts, they are rarely used in vehicular and mobile applications. Typical heights of microstrip antennas

Specification	Value
Frequency band	1164–1610 MHz
Polarization	RHCP
Input impedance	50 Ohm
VSWR	<2.5 (typical)
Gain at 0° (zenith)	Min 0 dBic
HPBW	85°–100° (typical)
Axial ratio (zenith)	<3 dB
Phase-centre stability	<10 mm

Table 2. GNSS antenna specifications.

for GNSS are 2–5 mm and can be designed on low or high dielectric substrates. Depending on substrate choice, the transverse dimensions range from 15 to 35 mm. One of the most commonly used form of microstrip antennas is ceramic dielectric with relative permittivity around 20, and overall size is typically 25×25 mm. This particular size and antenna performance match very well for most vehicle tracking and navigation applications. Many automobiles utilize this size for their information and navigation unit. The design of microstrip antennas is well documented in text books. Resonating patch dimension is made half of the guided wavelength and TM_{01} and TM_{10} modes are both excited with 90° phase difference with proper excitation and slight difference between electrical lengths that correspond to respective modes. Fractional and axial ratio bandwidths are usually small but tolerable for L1 band GPS and Galileo. For entire upper L-band, axial ratio is usually compromised for impedance bandwidth and most ceramic patches are linearly polarized than RH circular for 51 MHz bandwidth of upper L-band.

Typical ceramic patches and dimensions of 25×25 mm ceramic patch for GPS L1 band are shown in **Figure 1**. This particular patch is modeled on 70×70 mm ground plane and simulated using CST Microwave Studio [42]. The results are displayed in **Figures 2–4**. Although the impedance bandwidth (VSWR < 2.5) is 35 MHz, its axial ratio bandwidth is only 8 MHz. Elevation cut along $\phi = 0$ plane also indicates that the axial ratio becomes larger than 3 dB at low elevations, in fact, it becomes linear vertically polarized, which makes it more susceptible to terrestrial jammers. Nevertheless, its peak gain of 5 dBic and HPBW of 100° at 1575.4 MHz, are quite acceptable for automobile and mobile applications, which is why it has been so popular among automotive OEMs. Measured performance is expected to be slightly worse than the simulations. The patch antenna is also ground plane size-dependent. For smaller ground planes, although peak gain is higher, HPBW gets narrower, and axial ratio performance especially at low elevations deteriorates considerably.

2.3. Helical antennas

Helical antenna, since its invention by J.D. Krauss, has become the prime choice for circular polarization due its excellent axial ratio bandwidth and ease of construction. When the

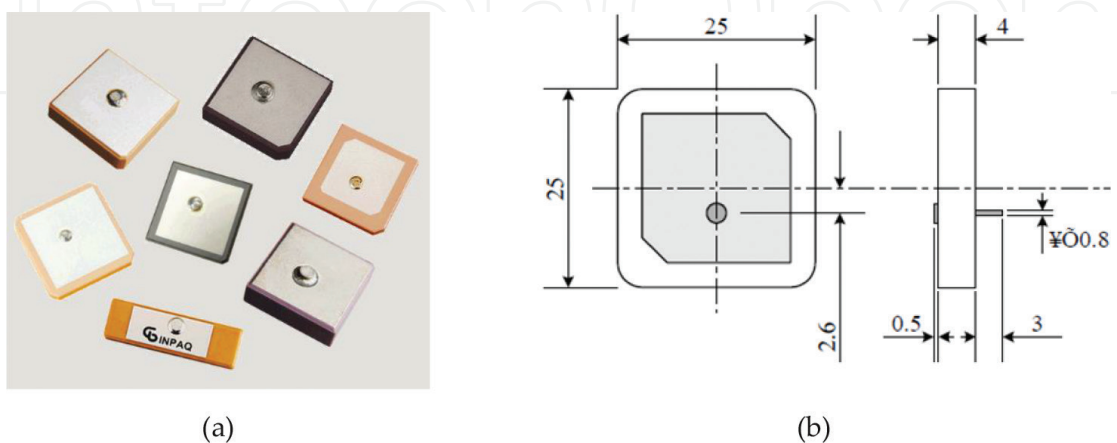


Figure 1. Ceramic GNSS patch antennas. (a) Inpaq [43] and (b) 25×25 mm patch by Amotech [44].

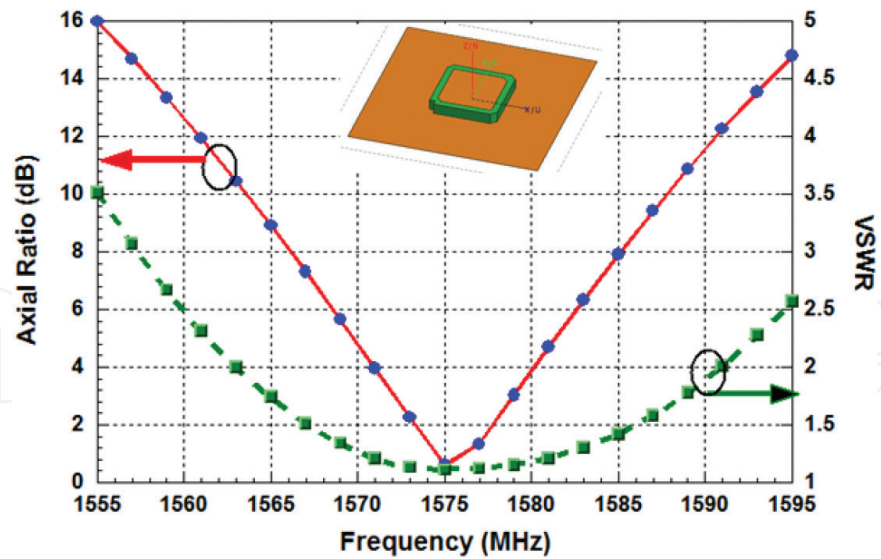


Figure 2. Axial ratio and VSWR of 25 × 25 mm ceramic patch on 70 × 70 mm ground plane.

diameter of the helix is in the order of operation wavelength, the antenna becomes circularly polarized with broadside radiation, and the rotation sense of helix provides the sense of polarization either left hand or right hand. This mode of operation is designated as axial mode. The axial ratio becomes smaller as the number of turns is increased. However, at GNSS bands, the wavelength is too large for the helical antenna to be of practical use for integration into a user platform. If smaller diameter is used, the antenna acts like a wire antenna, and this mode of operation is termed as normal mode. To obtain circular polarization, four helices with 90° apart geometrically are fed with 90° successive phase differences. This particular form of the antenna

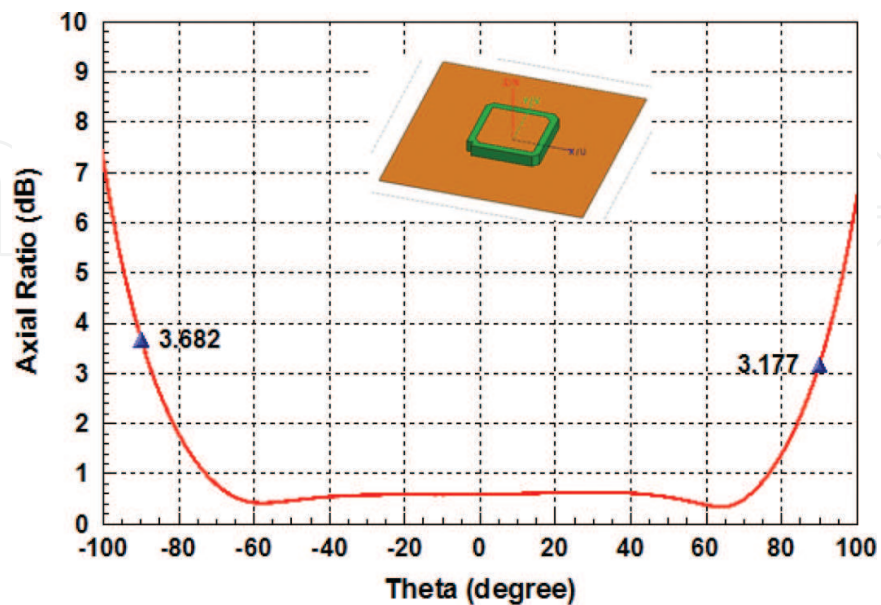


Figure 3. Axial ratio on phi = 0 cut for 25 × 25 mm ceramic patch on 70 × 70 mm ground plane at 1575.4 MHz.

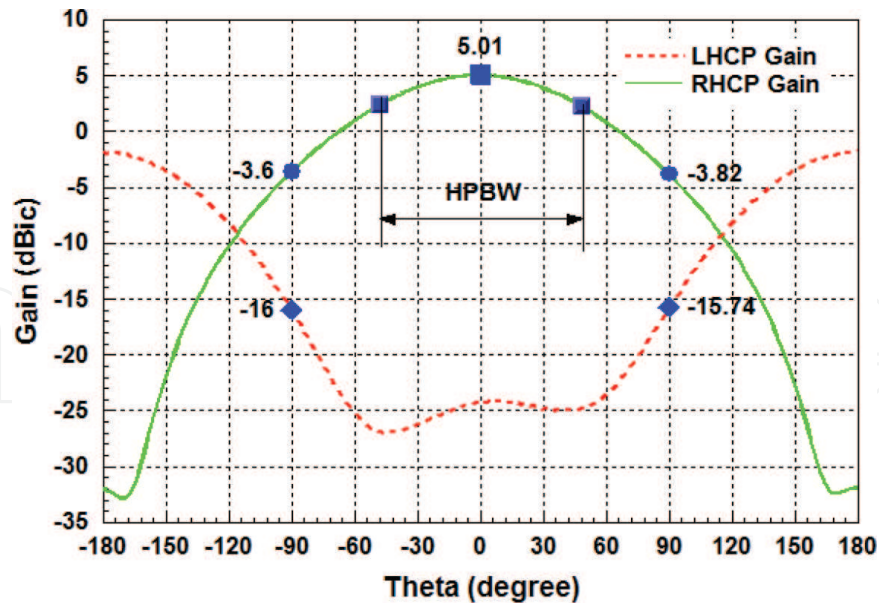


Figure 4. RHCP and LHCP gain of 25×25 mm ceramic patch on 70×70 mm ground plane at 1575.4 MHz.

is known as quadrifilar helical antenna (QHA) and has been heavily used due to its superior performance compared to patch antennas, especially wider axial ratio bandwidth. The size of the antenna can be reduced by printing helical arms on high dielectric constant ceramic substrate. The helical arms can also be implemented on flexible thin substrates. These two forms of helical antennas are shown in Figure 5. Most QHA designs utilize a quadrature hybrid coupler to feed the four arms of the antenna. In these designs, the bandwidth of the quadrature coupler is usually the limiting factor in achieving wide axial ratio bandwidth rather than the antenna structure itself. For instance, upper L-band GNSS can be entirely covered with QHA if an appropriate quadrature coupler is used. Quadrature couplers designed on low-temperature co-fired ceramic (LTCC) substrate provide chip-size dimensions but have narrow bandwidth due to high dielectric constant used.



Figure 5. Quadrifilar helical antenna: (a) printed on foil (Harxon HX-CH6017A [45]) and (b) printed on dielectric ceramic (Serantel [46]).

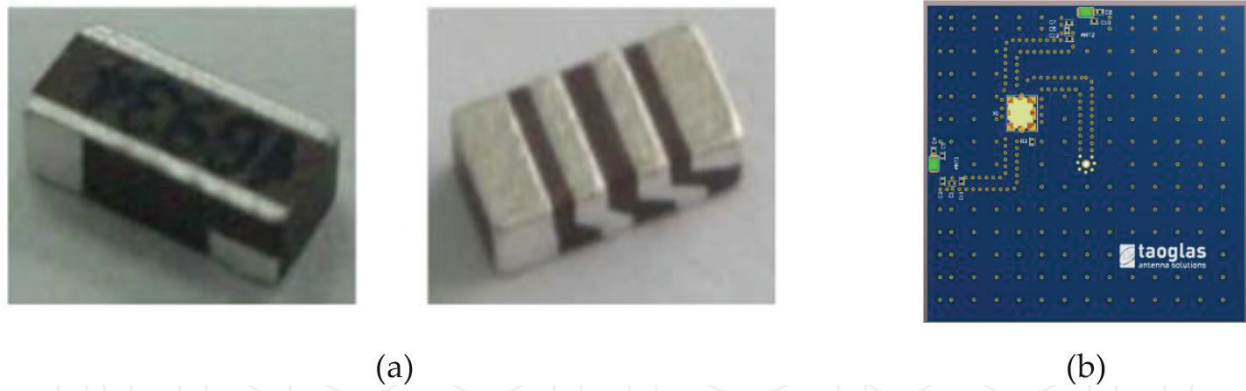


Figure 6. Chip antenna. (a) Monopole and helix by Abracon [47] and (b) Taoglass MAT.12A dual-chip antenna fed with a quadrature coupler [48].

2.4. Miniature antennas

Miniature antennas in several millimetre scales are often used in highly integrated consumer products. Their polarization is linear and average gains are usually less than -2 dBi even with large ground planes underneath. Different types of chip antennas in the form of monopoles and helix are shown in **Figure 6a**. In an attempt to improve their performance, Taoglass offered two chip antennas oriented perpendicular to each other and fed by a quadrature coupler as illustrated in **Figure 6b**.

2.5. High-performance antennas

High-precision GNSS systems require best antenna performance in terms of good axial ratio at low elevation angles, high rejection to multipath signals and minimum phase centre variation, and very high front-to-back ratio. Measured characteristics of these antennas are also integrated into the calibration of the GNSS receiver system. To achieve sub-centimetre accuracy, these antennas often supplemented with augmentation systems which provide local correction factors in pseudo-range estimates. These antennas also play an important role for rover applications as two-way communication outside the GNSS band is established between the units. Choke rings and artificial magnetic conductors are used to increase multipath rejection by maintaining good axial ratio even below the horizon of the antenna plane. Two different choke rings are illustrated in **Figure 7** by Leica Systems [49].

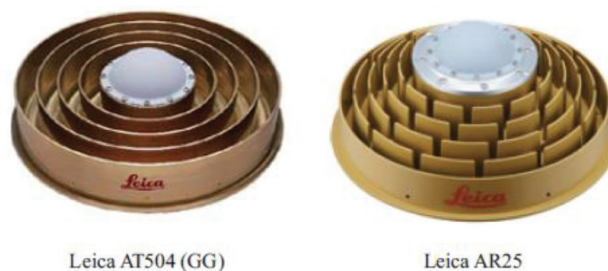


Figure 7. Leica choke-ring antennas [49].

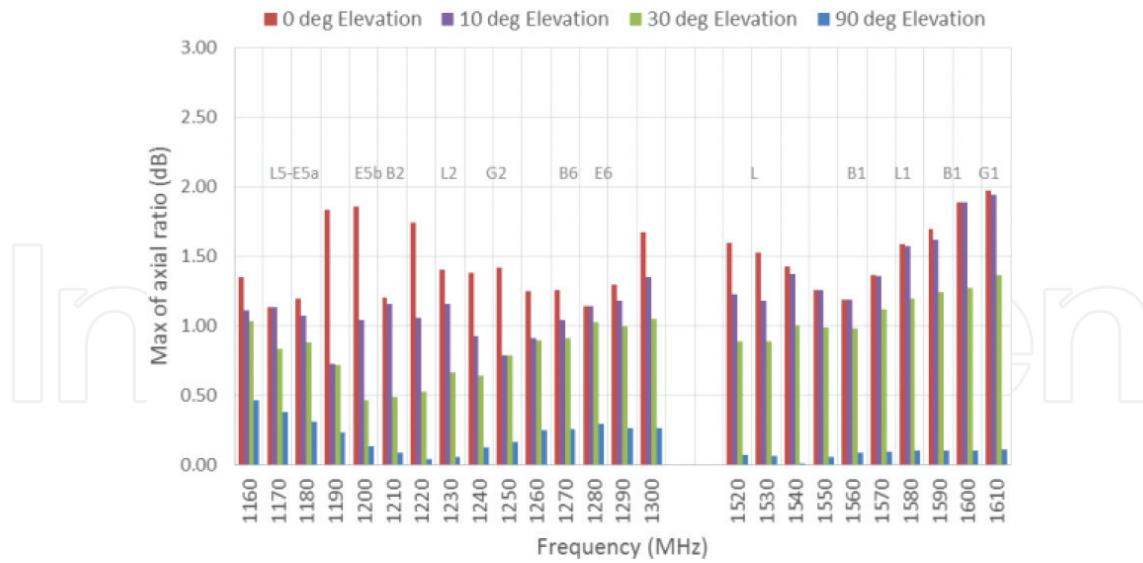


Figure 8. Axial Ratio of VeraPhase™ 6000 antenna by Tallysman Wireless Inc. [50].

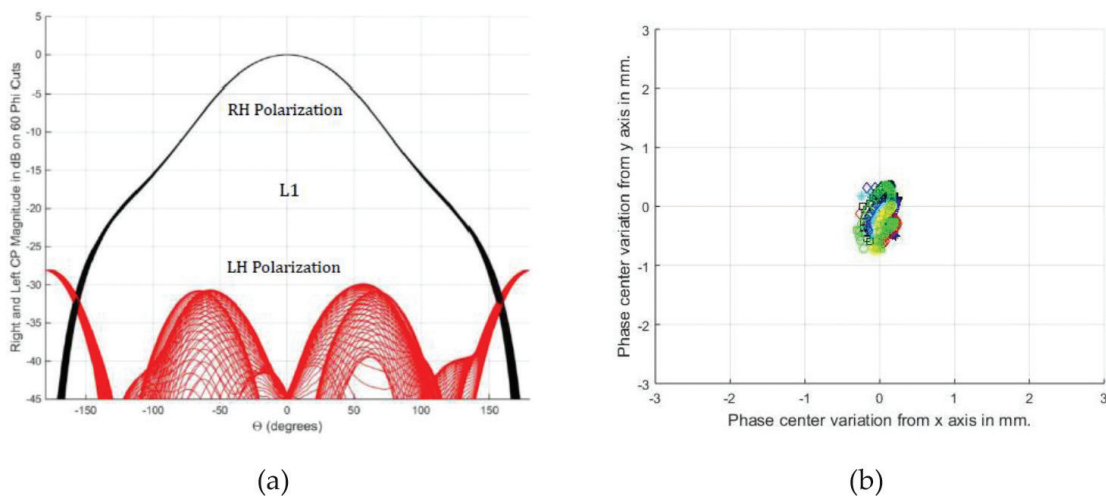


Figure 9. VeraPhase™ 6000 antenna by Tallysman Wireless Inc. (a) normalized RHCP and LHCP gain patterns and (b) phase centre variation [50].

Performances of Tallysman VeraPhase 6000 antenna [50] are shown in **Figures 8 and 9**. Axial ratio difference between 90° and at 0° elevation angles are about 1.5 dB, cross-polarization is less than -30 dB on antenna plane, and phase centre variation in horizontal plane is around 1 mm.

3. GNSS antenna LNA

LNA is an essential component of any satellite system [51, 52]. Typical strength of received GNSS signal is around 0.14 μV peak (-127 dBm for 50 Ohm), as mentioned earlier well below the thermal noise floor (-101 dBm for 20 MHz antenna bandwidth, i.e. 2.82 μV-peak). Received signal buried in noise, must be amplified all the way up to 1 V peak-to-peak for analog-digital

conversion (ADC) with minimal distortion. Most GNSS receivers utilize a low noise amplifier (LNA) connected to the passive antenna. This LNA is critical in determination of system noise figure, which is a measure of signal-to-noise ratio (SNR) degradation when the signal passes through a component or device. Total noise figure of the receiver chain is calculated as:

$$NF = NF_1 + \frac{NF_1 - 1}{G_1} + \frac{NF_2 - 1}{G_1 G_2} + \dots \quad (3)$$

Hence, first amplifier's gain and noise figure are vital to the system noise figure. The gain of the first amplifier should be kept as high as possible but the noise figure as low as possible which are contradictory in nature. Usually manufacturers of low-noise transistors provide optimum source reflection coefficient (Γ_{opt}) for the best noise figure, which is different than the maximum transducer gain. LNA design with feedback topologies target achieving best of both metrics at the expense of additional components and circuit complexity. LNA gain should be carefully selected to overcome the cable loss between the antenna LNA and receiver input LNA. Too much gain at the antenna LNA may overload and compress the receiver LNA for degraded performance. If the antenna is close to the receiver, passive antenna can be directly connected to the receiver with noise figure of the first stage being only the antenna cable loss. This configuration is not preferred in practical applications simply because pre-filter for out-of-band rejection is usually added before the receiver LNA, and this, combined with the antenna cable loss, increases the noise figure. Alternative configuration is to have a 10–15 dB LNA gain for short and moderately long cables and 25–30 dB gain for long cables.

Although GNSS receiver exploits processing gain to increase received signal SNR, in-band and out-band interference can degrade the receiver performance. Out-of-band interference can be handled at the antenna LNA using highly selective bandpass filter. The location of this filter either before or after the first gain stage impacts the noise figure and system performance. Sources of out-of-band interferers vary but they are often attributed to cellular phone base stations, terrestrial broadcast towers, radars, where second- and third-order products of transmitted signals fall into GNSS band. For instance, terrestrial broadcast of satellite digital audio system (SDARS) at S band (2320–2345 MHz) mixed 800 MHz 2G/3G cellular band falls into upper L-band, or L-band secondary surveillance radar at airport traffic control can easily mix up with 350/433 MHz or trunked radio services produce second-order products at GNSS bands. In addition, strong out-of-band signals may compress the LNA and de-sense the receiver. Closely packed cellular phone antennas, if not carefully designed, may easily compress the input LNA at the antenna.

In-band interferers due to third-order products should also be taken into account to avoid non-linear operation of the LNA. Too much gain at the antenna LNA can easily produce third-order products that compress the receiver LNA.

Typical passive antenna and LNA configurations are shown in **Figure 10** where pre-filter is located before or after the first-stage LNA. Having filter before the first-stage amplifier increases selectivity of the receiver by suppressing out-of-band signals but at the same time increases the noise figure, which may become critical, especially reception from low elevation angles or in an urban setting. For nearby radiators to GNSS antenna, this configuration

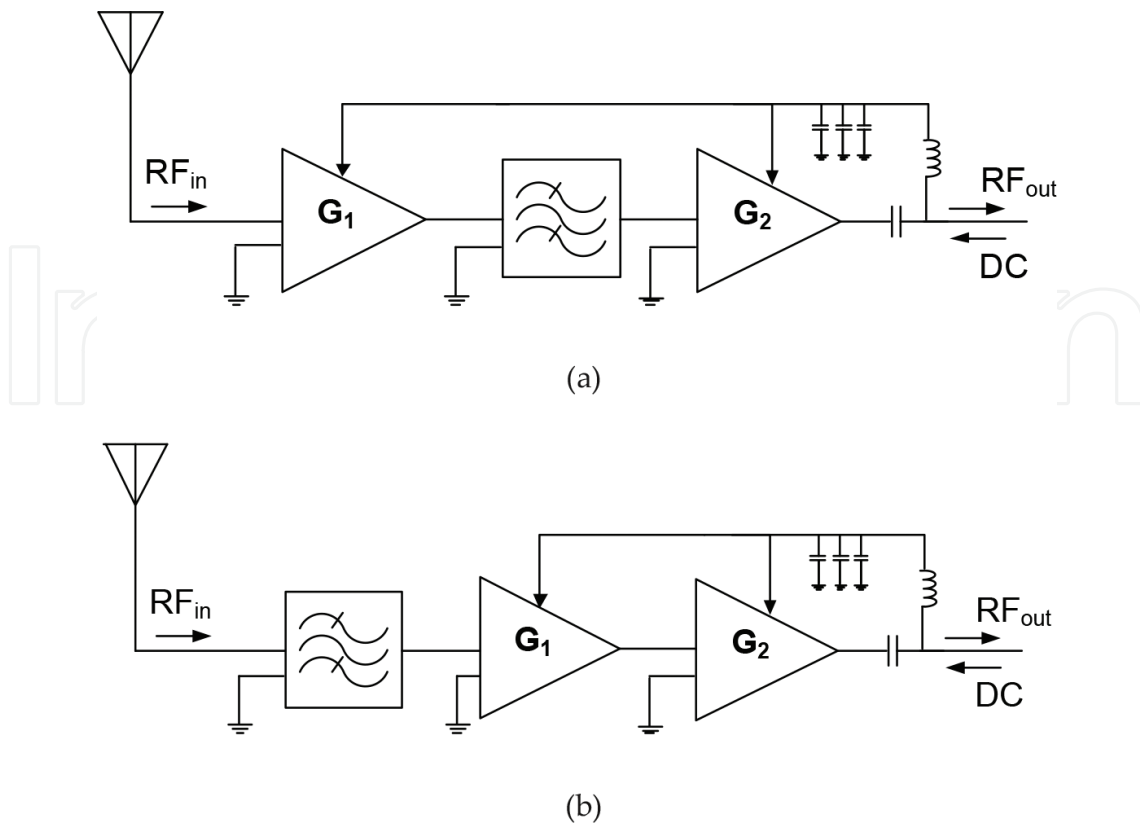


Figure 10. Antenna LNA: (a) filter after first stage and (b) filter before first stage.

is inevitable. Filter after the first-stage LNA does not degrade the noise figure much and provides good selectivity and rejection for out-of-band signals. However, in the presence of a strong interferer, antenna LNA can be overloaded and signal acquisition can be lost.

4. GNSS receiver front-end

GNSS receivers generally utilize RF down-conversion to an intermediate frequency (IF), using one or two conversions, followed by analog-to-digital conversion (ADC). The output of ADC is interfaced to a general purpose processor (GPP) for digital signal processing operations such as correlation, acquisition, tracking, and PNT extraction. The section where the signal remains analog, i.e. up to ADC, is usually termed as front-end. Receiver architectures based on how they process signal can be classified as superheterodyne, low IF, zero IF (homodyne), and direct-digital (bandpass sampling). Receiver performance metrics can be quite detailed but the most important ones are sensitivity, selectivity, inter-modulation characteristics, non-linearities, and spur-free dynamic range.

Superheterodyne receiver is the most classical architecture, and has been utilized in many communication systems due to its excellent sensitivity, selectivity, and dynamic range. Typical configuration is shown in **Figure 11**. However, the architecture is not flexible for

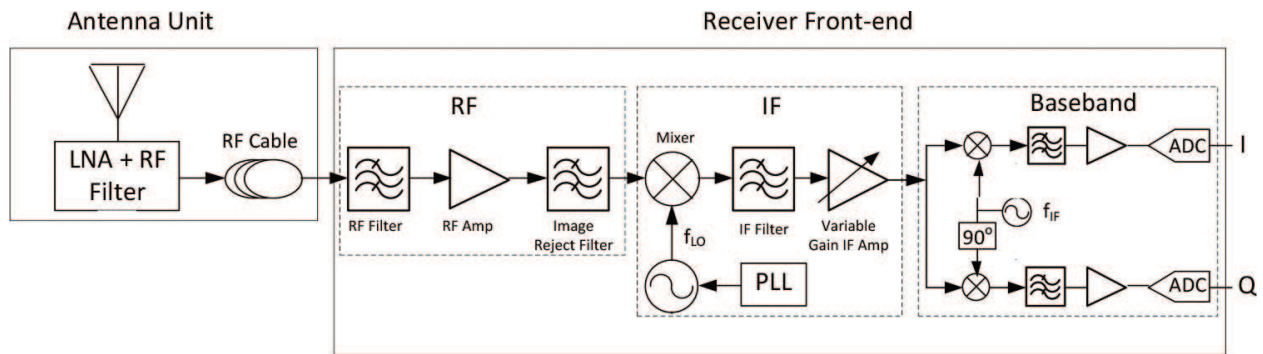


Figure 11. Antenna unit and superheterodyne receiver front-end.

multi-standard systems, not well suited for integrated circuits due to filter requirements for image-reject and non-linear products, and consumes substantial power.

To overcome the drawbacks of superheterodyne receiver, low-IF and zero-IF receiver configurations are proposed. Typical architecture of these receivers is displayed in **Figure 12**. In zero-IF configuration, image problem is completely removed, hence sharp and IC unfriendly image reject filters are not needed. Since gain is shared between RF and baseband amplifiers, requirements on these amplifiers become complicated to have sufficient SFDR. But, the most troubling problem of zero-IF is that the leakage of LO mixes with itself, putting severe requirements on second-order intermodulation products of the receiver. This leakage causes DC offsets at the baseband, and high baseband gain amplifies these offsets together with flicker noise to degrade receiver performance. Also, Doppler shifts of received signals can be lost. Low-IF configuration overcomes these problems but image issue comes up again and usually resolved by image-reject mixer design, which is not so easy in IC topology. Despite severe requirements on gain, noise, and linearity, low power budget and flexibility in DSP made these architectures very popular, especially among receiver ICs.

Today's multi-band and multi-constellation receivers mostly utilize software-defined radio architecture to process digital I and Q signals. When two or more frequencies of GNSS are targeted, the GPP unit of the receiver becomes critical for signal quality and high data throughput, which may require parallel processing of correlations [53]. In contrast to communication systems

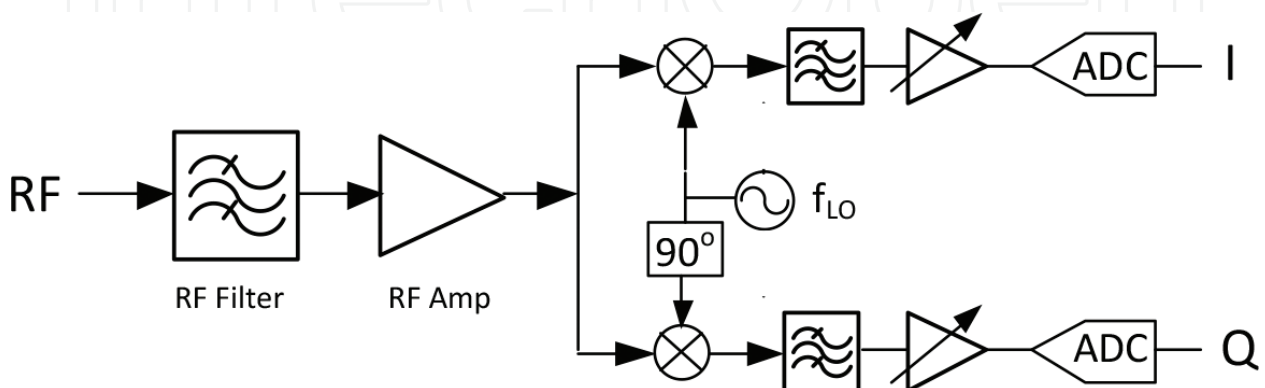


Figure 12. Zero-IF and low-IF receiver front-end. IF filters are either low-pass (zero-IF) or bandpass (low-IF).

where received signal SNR is high, GNSS receivers rely on long coherent integration (>1 ms) to exploit processing gain. Clock stability becomes an issue especially during carrier phase tracking. Instead of quartz oscillators, temperature-compensated crystal oscillators (TCXO) with an accuracy better than one part per million with very low phase noise are used in high-end receivers.

5. Conclusions

GNSS performance relies on the antenna, front-end receiver, and DSP algorithms utilized in the software. Antenna, being the first element in the reception chain, plays a key role in retrieving PNT information. Antenna specifications based on the expected performance of the GNSS receiver were reviewed and discussed in detail. Common forms of antennas ranging from high end to low-cost applications were presented. Front-end receiver configurations and elements were outlined for GNSS performance. Low-IF digital configuration was recommended for best receiver performance. This review should especially help algorithm developers in choosing the right antenna and receiver configuration.

Acknowledgements

This work is partly supported by Ege University BAP 16-MUH-032, and The Scientific and Research Council of Turkey (TUBITAK) under grant no: 1005.STZ.2015, and Vestel Electronics Inc., Manisa, Turkey.

Conflict of interest

None.

Author details

Korkut Yegin

Address all correspondence to: yegink@gmail.com

Ege University Electrical and Electronics Engineering, Izmir, Turkey

References

- [1] Huang C-Y, Lin M-H. Ceramic GPS antenna for remote sensing. IGARSS 2000. In: IEEE 2000 International Geoscience and Remote Sensing Symposium. 2000. pp. 2182-2184. DOI: 10.1109/IGARSS.2000.858349

- [2] Abraham O, Leib A, Matzner H. Designing and building of a circular GPS antenna. In: IEEE International Conference on Microwaves, Communications, Antennas and Electronic Systems. 2011. pp. 1-3. DOI: 10.1109/COMCAS.2011.6105835
- [3] Nasimuddin, Chen ZN, Qing X. Dual-band circularly polarized S-shaped slotted patch antenna with a small frequency-ratio. IEEE Transactions on Antennas and Propagation. 2010;58:2112-2115. DOI: 10.1109/TAP.2010.2046851
- [4] Bilotti F, Vegni C. Design of high-performing microstrip receiving GPS antennas with multiple feeds. IEEE Antennas and Wireless Propagation Letters. 2010;9:248-251. DOI: 10.1109/LAWP.2010.2046874
- [5] Boccia L, Amendola G, Di Massa G. A shorted elliptical patch antenna for GPS applications. IEEE Antennas and Wireless Propagation Letters. 2003;2:6-8. DOI: 10.1109/LAWP.2003.810767
- [6] Yegin K. On-vehicle GPS antenna measurements. IEEE Antennas and Wireless Propagation Letters. 2007;6:488-491. DOI: 10.1109/LAWP.2007.907056
- [7] Yegin K. Instrument panel mount GPS antenna. Microwave Optical Technology Letters. 2007;49:1979-1981
- [8] Scire-Scappuzzo F, Makarov SN. A low-multipath wideband GPS antenna with cutoff or non-cutoff corrugated ground plane. IEEE Transactions on Antennas and Propagation. 2009;57:33-46. DOI: 10.1109/TAP.2008.2009655
- [9] Yigit O, Yegin K. All band GNSS antenna with artificial magnetic conductor. In: 2017, Progress in Electromagnetic Research Symposium. 2017. pp. 2211-2214. DOI: 10.1109/PIERS.2017.8262118
- [10] Hong-mei Z, Yan-juan N, Teng L. A novel GPS antenna with wide beamwidth. In: 2010 2nd International Conference on Future Computer and Communication. 2010. pp. 49-52. DOI: 10.1109/ICFCC.2010.5497838
- [11] Brzezina G, Roy L. A miniaturized GPS antenna in LTCC with linear polarization suitable for SoP integration. In: 2010 14th International Symposium on Antenna Technology and Applied Electromagnetics & The American Electromagnetics Conference. 2010; pp. 1-4
- [12] Yue L, Chen CC, Psychoudakis D, Volakis JL. Miniaturized 1: Dual-band GPS antenna element. In: 2010 IEEE Antennas and Propagation Society International Symposium. 2010. pp. 1-4. DOI: 10.1109/APS.2010.5561178
- [13] Tang TC, Tsai CH, Lin KH, Huang YT, Chen CY. Fractal GPS antenna design on piezoelectric substrate. In: 2010 Asia-Pacific Microwave Conference. 2010. pp. 991-994
- [14] Park J, Choi J, Lee TH, Kim YS. Small GPS antenna with lumped elements and interdigital structure. IEEE Radio and Wireless Symposium. 2012:55-58. DOI: 10.1109/RWS.2012.6175393

- [15] Vallozzi L, Vandendriessche W, Rogier H, Hertleer C, Scarpello ML. Wearable textile GPS antenna for integration in protective garments. In: Proceedings of the Fourth European Conference on Antennas and Propagation. 2010. pp. 1-4
- [16] Mariottini F, Albani M, Toniolo E, Amatori D, Maci S. Design of a Compact GPS and SDARS integrated antenna for automotive applications. *IEEE Antennas and Wireless Propagation Letters*. 2010;**9**:405-408. DOI: 10.1109/LAWP.2010.2049632
- [17] Yap MS, Ng L, Aditya S. A triple band antenna for GSM and GPS application. In: Fourth International Conference on Information, Communications and Signal Processing, and the Fourth Pacific Rim Conference on Multimedia. 2003. pp. 1119-1123. DOI: 10.1109/ICICS.2003.1292634
- [18] Bilgic MM, Yegin K. Modified annular ring antenna for GPS and SDARS automotive applications. *IEEE Wireless and Propagation Letters*. 2016;**15**:1442-1445. DOI: 10.1109/LAWP.2015.2512558
- [19] Wang M, Deng X, Gu C. Tri-band GPS antenna with low-multipath ground plane. In: 2010 International Symposium on Signals, Systems and Electronics. 2010. pp. 1-4
- [20] Basilio LI, Chen RL, Williams JT, Jackson DR. A new planar dual-band GPS antenna designed for reduced susceptibility to low-angle multipath. *IEEE Transactions on Antennas and Propagation*. 2007;**55**:2358-2366. DOI: 10.1109/TAP.2007.901818
- [21] Lee Y, Ganguly S, Mittra R. Multi-band L5-capable GPS antenna with reduced backlobes. In: *IEEE Antennas and Propagation Society International Symposium*. 2005. pp. 438-441
- [22] Zhou Y, Chen CC, Volakis JL. A single-fed element antenna for tri-band anti-jamming GPS arrays. In: *IEEE Antennas and Propagation Society International Symposium*. 2008. pp. 1-4
- [23] Zhou Y, Chen CC, Volakis JL. Dual band proximity-fed stacked patch antenna for tri-band GPS applications. *IEEE Transactions on Antennas and Propagation*. 2007;**55**:220-223. DOI: 10.1109/TAP.2006.888476
- [24] Zhou Y, Koulouridis S, Kiziltas G, Volakis JL. A novel 1.5 quadruple antenna for tri-band GPS applications. *IEEE Antennas and Wireless Propagation Letters*. 2006;**5**:224-227. DOI: 10.1109/LAWP.2006.875282
- [25] Boccia L, Amendola G, Di Massa G. A high performance dual frequency microstrip antenna for global positioning system. *IEEE Antennas and Propagation Society International Symposium*. 2001. pp. 66-69
- [26] Zhang X, Ma X, Lai Q. Two kind of conical conformal GPS antenna arrays on projectile. In: 2009 3rd IEEE International Symposium On Microwave, Antenna, Propagation and EMC Technologies for Wireless Communications. 2009. pp. 659-662
- [27] Zhang X, Ma X, Guan X. Design of cylindrical conformal microstrip GPS antenna arrays. In: *International Conference on Microwave Technology and Computational Electromagnetics*. 2009. pp. 105-108

- [28] Bang JH, Enkhbayar B, Min DH, Ahn BC. A compact GPS antenna for artillery projectile applications. *IEEE Antennas and Wireless Propagation Letters*. 2011;**10**:266-269. DOI: 10.1109/LAWP.2011.2135830
- [29] Lingling Z, Jinghui Q, Bo S. Design of GPS antenna array on revolving cylinder. In: 2007 Asia-Pacific Microwave Conference. 2007. pp. 1-4
- [30] Wu K, Zhang L, Shen Z, Zheng B. An anti-jamming 5-element GPS antenna array using phase-only nulling. In: 6th International Conference on ITS Telecommunications. 2006. pp. 370-373
- [31] Kuester C, Chaloupka H, Knauth J. A high temperature superconducting anti-jam GPS antenna array. In: MILCOM 1999. 1999. pp. 671-674. DOI: 10.1109/MILCOM.1999.822768
- [32] Kasemodel JA, Chen CC, Gupta IJ, Volakis JL. Miniature continuous coverage wide-band GPS antenna array. In: IEEE Antennas and Propagation Society International Symposium. 2008. pp. 1-4. DOI: 10.1109/APS.2008.4619966
- [33] Fernandez Prades C, Closas Gomez P, Fernandez Rubio JA. New trends in global navigation systems: Implementation of a GPS antenna array receiver. In: Proceedings of the Eighth International Symposium on Signal Processing and Its Applications. 2005. pp. 903-906. DOI: 10.1109/ISSPA.2005.1581085
- [34] Gupta IJ. Non-planar adaptive antenna arrays for GPS receivers. *IEEE Antennas and Propagation Magazine*. 2010;**52**:35-51. DOI: 10.1109/MAP.2010.5687504
- [35] Sisman I, Yegin K. Reconfigurable antenna for jamming mitigation of legacy GPS receivers. *International Journal of Antennas and Propagation*. 2017; Article ID 4563571. DOI: 10.1155/2017/4563571
- [36] Hsu WH, Pan SC, Huang YT. A well placement design to improve GSM/DCS and GPS antenna isolation. In: Proceedings of the 9th International Symposium on Antennas, Propagation and EM Theory. 2010. pp. 8-11. DOI: 10.1109/ISAPE.2010.5696381
- [37] Yegin K. AMPS/PCS/GPS active antenna for emergency call systems. *IEEE Antennas and Wireless Propagation Letters*. 2007;**6**:255-258. DOI: 10.1109/LAWP.2007.897510
- [38] Zhu N, Ziolkowski RW. Metamaterial-inspired, near-field resonant parasitic GPS antennas: Designs and experiments. In: IEEE International Symposium on Antennas and Propagation. 2011. pp. 658-660
- [39] Pigeon M, Morlaas C, Aubert H. A dual-band high impedance surface mounted with a spiral antenna for GNSS applications. In: IEEE-APS Topical Conference on Antennas and Propagation in Wireless Communications. 2011. pp. 994-997
- [40] Bao XL, Ruvio G, Ammann MJ, John M. A novel GPS patch antenna on a fractal hi-impedance surface substrate. *IEEE Antennas and Wireless Propagation Letters*. 2006;**5**:323-326. DOI: 10.1109/LAWP.2006.878900
- [41] Yigit O, Akkaya İ, Oztürk Y, Yegin K. Plasma frequency selective surface for GPS application. In: 2017, TELFOR Conference; Belgrade, Serbia

- [42] CST Microwave Studio AG, Germany. 2017. www.cst.com [Accessed: 26.12.2017]
- [43] Inpaq. Ceramic GNSS Patches [Internet]. 2017. www.inpaq.com [Accessed: 26.12.2017]
- [44] Amotech. Ceramic GNSS Patches [Internet]. 2017. www.amotech.com [Accessed: 26.12.2017]
- [45] Harxon. HX-CH6017A [Internet]. 2017. www.harxon.com [Accessed: 26.12.2017]
- [46] Serantel. QHA Antenna 2017. www.farnell.com [Accessed: 26.12.2017]
- [47] Abracon. Chip antennas [Internet]. 2017. www.abracon.com [Accessed: 26.12.2017]
- [48] Taoglass. MAT.12A dual-chip antenna [Internet]. 2017. www.taoglass.com [Accessed: 26.12.2017]
- [49] Leica. AT 504 and AR 25 [Internet]. 2017. www.leica.com [Accessed: 26.12.2017]
- [50] Tallysman Wireless Inc. VeraPhase™ 6000 [Internet]. 2017. www.tallysman.com [Accessed: 26.12.2017]
- [51] Yegin K. Design an ultra low-noise S-band amplifier. *Electronic Design News*. June 7, 2012
- [52] Yegin K. On-glass automotive diversity antenna and LNA design for S-band satellite digital radio. *International Journal of Electronics*. 2015;**102**:1804-1817. DOI: 10.1080/00207217.2014.996783
- [53] Curran JT, Fernández-Prades C, Morrison A, Bavaro M. Innovation: The continued evolution of the GNSS software-defined radio. *GPS World*. 2018